

Downregulation of lamin A by tumor suppressor AIMP3/p18 leads to a progeroid phenotype in mice

Young Sun Oh,¹ Dae Gyu Kim,¹ Gyuyoung Kim,¹ Eung-Chil Choi,¹ Brian K. Kennedy,² Yousin Suh,³ Bum Joon Park⁴ and Sunghoon Kim^{1,5}

¹Center for Medicinal Protein Network and Systems Biology, College of Pharmacy, Seoul National University, Seoul 151-742, Korea

²Department of Biochemistry, University of Washington, Seattle, WA 98195, USA

³Departments of Medicine and Genetics, Albert Einstein College of Medicine, Bronx, NY 10461, USA

⁴Department of Molecular Biology, College of Natural Science, Pusan National University, 30 Jangjeon-dong, Geumjeong-gu, Busan 609-735, Korea

⁵Department of Molecular Medicine and Biopharmaceutical Sciences, Graduate School of Convergence Technology, Seoul National University, Suwon 443-270, Korea

Summary

Although AIMP3/p18 is normally associated with the macromolecular tRNA synthetase complex, recent reports have revealed a new role of AIMP3 in tumor suppression. In this study, we generated a transgenic mouse that overexpresses AIMP3 and characterized the associated phenotype *in vivo* and *in vitro*. Surprisingly, the AIMP3 transgenic mouse exhibited a progeroid phenotype, and the cells that overexpressed AIMP3 showed accelerated senescence and defects in nuclear morphology. We found that overexpression of AIMP3 resulted in proteasome-dependent degradation of mature lamin A, but not of lamin C, prelamin A, or progerin. The resulting imbalance in the protein levels of lamin A isoforms, namely altered stoichiometry of prelamin A and progerin to lamin A, appeared to be responsible for a phenotype that resembled progeria. An increase in the level of endogenous AIMP3 has been observed in aged human tissues and cells. The findings in this report suggest that AIMP3 is a specific regulator of mature lamin A and imply that enhanced expression of AIMP3 might be a factor driving cellular and/or organismal aging.

Key words: aging; AIMP3/p18; LaminA; progeroid; tumor suppressor.

Introduction

Aminoacyl-tRNA synthetases (ARSs) in higher eukaryotes form a unique macromolecular complex that consists of nine different enzymes and three auxiliary factors termed aminoacyl-tRNA synthetase-interacting multifunctional proteins (AIMPs) (Park *et al.*, 2005b). Diverse functions and diseases have been attributed to many of the ARSs and AIMPs that are involved in this complex (Park *et al.*, 2008). In addition to being the smallest component of the multi-tRNA synthetase complex (Han *et al.*, 2006), AIMP3 is activated in response to DNA damage (Park *et al.*, 2005a) and oncogenic stimuli (Park *et al.*, 2006), which result in its translocation to the nucleus, where it activates p53 via an interaction with ATM (Ataxia Telangiectasia Mutated) and ATR (Ataxia Telangiectasia and Rad3-related). Allelic deletions (Park *et al.*, 2005a) or point mutations (Kim *et al.*, 2008) of AIMP3 that inactivate or reduce its ability to activate p53 are observed in patients with cancer. Whereas mice that are homozygous null for AIMP3 showed early embryonic death, heterozygous mice are born alive but show highly increased susceptibility to various cancers (Park *et al.*, 2005a). AIMP3 heterozygous cells that are transformed with oncogenes such as Ras or Myc also displayed severe nuclear fragmentation and chromosome instability (Park *et al.*, 2006).

Cellular senescence serves as a major mechanism of tumor suppression (Collado *et al.*, 2005, 2007). Based on aforementioned evidence that AIMP3 is a potent tumor suppressor, in the study described herein, we tested and confirmed the hypothesis that overexpression of AIMP3 leads to cellular senescence. Moreover, we generated and characterized AIMP3 transgenic mice and found that they have a significantly shorter lifespan than wild-type mice and show characteristics common to murine models of progeria.

Among the mutations that are associated with progeria are dominant mutations in *LMNA* (encoding A-type lamins), which cause Hutchinson–Gilford progeria syndrome (HGPS) (De Sandre-Giovannoli *et al.*, 2003; Eriksson *et al.*, 2003). The *LMNA* gene encodes two primary spliced forms in somatic cells (lamin A and C), which arise by alternate splicing (Fisher *et al.*, 1986; McKeon *et al.*, 1986). Unlike lamin C, lamin A contains a unique C-terminus that ends in the residues CaaX (a = aliphatic), which dictate farnesylation on the cysteine residue (Fisher *et al.*, 1986; Reid *et al.*, 2004; Rusinol & Sinensky, 2006). Lamin A is farnesylated transiently, after which the endopeptidase ZMPSTE24 mediates a cleavage event that removes the C-terminus, including the CaaX motif, to generate mature lamin A (Pendas *et al.*, 2002; Dechat *et al.*, 2008). The most common mutations in *LMNA* that are associated with progeria promote altered splicing and generate a third polypeptide, progerin, that lacks 50 amino

Correspondence

Sunghoon Kim, Center for Medicinal Protein Network and Systems Biology, College of Pharmacy, Seoul National University, Seoul 151-742, Korea.
Tel.: 82-2-880-8180; fax: 82-2-875-2621; e-mail: sungkim@snu.ac.kr

Accepted for publication 12 July 2010

acids, which include the internal ZMPSTE24 cleavage site, and thus remains permanently farnesylated (De Sandre-Giovannoli et al., 2003; Eriksson et al., 2003). Permanent farnesylation of this polypeptide contributes to disease, because inactivating mutations in ZMPSTE24 that result in permanent farnesylation of prelamin A give rise to a set of progeroid disorders that are also associated with mutations in LMNA (Pendas et al., 2002; Agarwal et al., 2003; Navarro et al., 2004).

Surprisingly, we found that cells in culture or mice overexpressing AIMP3 showed enhanced proteasome-dependent degradation of lamin A, but not of lamin C, unprocessed lamin A or progerin. Underlying this specificity for mature lamin A, AIMP3 interacted with and recruited the ubiquitin ligase, Siah1, to lamin A but failed to bind progerin or lamin C because the C-terminal region that is lacking in progerin or lamin C was required for the interaction. Collectively, these findings lead to a model whereby AIMP3 promotes a phenotype that is associated with progeria by altering the relative levels of A-type lamin isoforms.

Results

Overexpression of AIMP3 promotes senescence

When activated by DNA damage or oncogenic stimuli, one mechanism by which AIMP3 might act as a tumor suppressor is by the promotion of cellular senescence. To test this possibility, we transfected HEK293 cells with plasmids for GFP-AIMP3 and GFP alone (control) and monitored the effects of AIMP3 on cell growth. Whereas the control cells showed continuous growth, as determined by the increase in the number of the GFP-transfected cells and the cell count, the growth of AIMP3 transfectants was significantly retarded (Fig. 1a,b). GFP-AIMP3 transfectants showed decreased residence in S phase and a compensatory increase in G0/G1 phase as they were cultured, which further suggests an antiproliferative activity of AIMP3 (Fig. 1c). Given that AIMP3 can activate p53 in response to DNA damage, via ATM and ATR (Park et al., 2005a), and that the

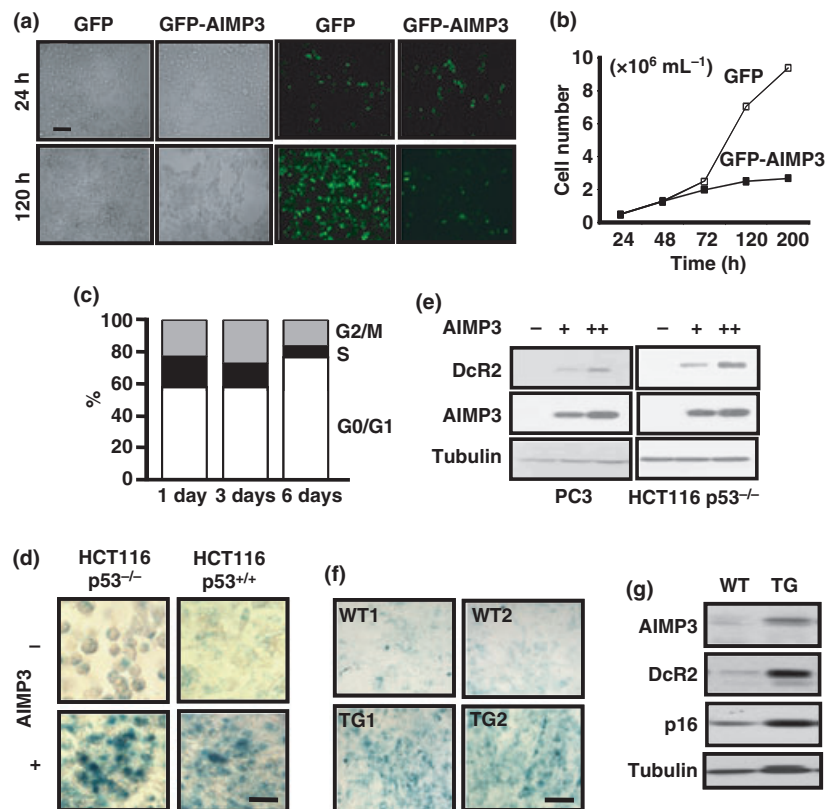


Fig. 1 AIMP3 suppresses proliferation and induces cellular senescence. (a) Bright-field (left panel) and fluorescence (right panel) microscopy images of 293 cells expressing GFP and GFP-AIMP3 at the indicated times after transfection. (Bar = 10 μm). (b) Growth curves of 293 cells expressing GFP and GFP-AIMP3. (c) Cell cycle profiles of 293 cells expressing GFP-AIMP3. Nuclei isolated from cells at the indicated times following expression of GFP-AIMP3 were stained with propidium iodide and analyzed by flow cytometry. The vertical axis indicates the percentage of cells in the G0–G1, S, and G2–M phases of the cell cycle (20 000 events were acquired per sample). (d) The effect of AIMP3 (+ indicates 6 μg mL⁻¹ of AIMP3-encoding plasmid) on senescence-associated β-galactosidase activity was determined by X-gal staining in p53^{+/+} and p53^{-/-} HCT116 cells. (Scale bar = 20 μm, magnification ×20) (e) The effect of AIMP3 on DcR2 levels was also determined by western blotting of DcR2 in p53-inactive PC3 and HCT116 cells (+ and ++ indicate 2 and 4 μg mL⁻¹ AIMP3 plasmid, respectively). (f) β-galactosidase staining of AIMP3 WT and TG mouse embryonic fibroblast cells after the serial passage of 8. (Scale bar = 20 μm, magnification ×20) (g) Immunoblot analysis of AIMP3 and senescence markers DcR2 and p16 in heart cells obtained from AIMP3 WT and TG mice.

activated p53 can induce senescence as well as cell death (Tyner *et al.*, 2002), we investigated whether AIMP3 induces cellular senescence in a p53-dependent manner. We transfected the AIMP3 expression construct into p53^{+/+} and p53^{-/-} HCT116 cells and determined whether AIMP3 could induce cellular senescence as measured by senescence-associated β -galactosidase activity (Dimri *et al.*, 1995). AIMP3 transfection increased β -galactosidase activity in both p53^{-/-} and p53^{+/+} HCT116 cells to a similar degree (Fig. 1d). To confirm this observation further, we introduced AIMP3 into two different cell lines, namely p53-inactive PC3 (Shappell *et al.*, 2001) and HCT116 cells, and monitored senescence by determining the cellular level of DcR2, which is another known marker of senescence (Sun *et al.*, 2007). The level of DcR2 was increased by the introduction of AIMP3 in both types of cell in a dose-dependent manner (Fig. 1e), providing further evidence the p53-independent induction of cellular senescence by AIMP3.

To determine whether the cellular senescence induced by AIMP3 can take place *in vivo*, we generated transgenic (TG) mice that express AIMP3 constitutively at higher level than wild-type controls. A cDNA encoding mouse AIMP3 was inserted into an expression vector that contained a chicken β -actin promoter (Kim *et al.*, 2002b) (Fig. S1a) and was used to generate a transgenic mouse as described in the Methods. The integration of the exogenous AIMP3 cDNA into the FVB/N mouse chromosome was confirmed by genomic PCR using different primer pairs (Fig. S1b,c,f). The elevated expression of AIMP3 in the TG mice was verified by both western blotting with a specific antibody and RT-PCR (Fig. S1d,e).

When β -galactosidase activity was compared by X-gal staining in mouse embryonic fibroblasts (MEFs) from the AIMP3 WT and TG mice, the AIMP3 TG cells showed higher staining than the WT cells (Fig. 1f). Conversely, the β -galactosidase activity was reduced when AIMP3 transcript was suppressed by its specific siRNA (Fig. S2). We also isolated heart cells from the mice and compared the senescence markers, DcR2 and p16 (Sun *et al.*, 2007; Swarbrick *et al.*, 2008), by western blotting. Again, the cells of AIMP3 TG mice showed a higher level of DcR2 and p16 than those of the WT littermates (Fig. 1g).

AIMP3 transgenic mice exhibit a progeroid phenotype

We examined whether the cellular senescence induced by elevated expression of AIMP3 is linked to the phenotype of AIMP3 TG mice. Although AIMP3 TG mice were born alive, they stopped gaining weight much earlier than their WT littermates (Fig. 2a), and the TG mice also showed enhanced mortality compared to the WT littermates (Fig. 2b). The TG mice also displayed alopecia (Fig. 2c,d), wrinkled skin with reduced adipocytes (Fig. 2e), lordokyphosis (Fig. 2f), reduced bone mineral deposits in female (Fig. 2g), and reduced bone thickness (Fig. 2h). This phenotype is characteristic of mouse progeroid models.

Expression of AIMP3 correlates inversely with lamin A levels

We sought to address the p53-independent mechanisms by which AIMP3 expression promotes cell senescence and the progeroid phenotype. Given that mutations in *LMNA*, which encodes A-type nuclear lamins, are linked to progeria, we considered the possibility that activated AIMP3 might translocate to the nucleus and affect the function of A-type lamin function in some manner. Nuclear deformation is a sign of altered function of A-type lamin and is also associated with cellular senescence (Verstraeten *et al.*, 2007; Dechat *et al.*, 2008). Therefore, we monitored the appearance of nuclei with altered morphology in HeLa cells transfected with the AIMP3 expression construct using antibodies to lamin A, which forms a latticework structure between the nuclear envelope and the underlying chromatin. The percentage of cells with deformed nuclear structure was increased to approximately 57% when the cells were transfected with the plasmid for AIMP3, whereas only 8% of the control cells showed nuclear deformation (Fig. 3a). To confirm this observation further, we also monitored the response of lamin A to AIMP3 by co-transfection of the expression vector for GFP-lamin A with that for AIMP3 or empty vector. Again, after transfection with the AIMP3 expression construct, approximately 63% of the cells showed disrupted nuclear morphology with the formation of GFP-lamin A nuclear foci, whereas similar morphology was observed at approximately 9% of the control cells (Fig. 3b).

Given that transfection of the AIMP3 expression construct induced nuclear deformation, we checked by the use of western blotting with an antibody specific to lamin A whether the levels of lamin A were altered in AIMP3 TG MEF cells. We found that the level of lamin A was reduced in AIMP3 TG cells compared with that in the WT cells (Fig. 3c). The senescence of MEFs that was induced by AIMP3 was rescued by exogenous supplementation of lamin A (Fig. S3), which indicates a functional association of AIMP3 with lamin A in the control of cellular senescence. Immunohistochemical analysis of lamin A in the skin of AIMP3 transgenic mice also revealed decreased levels of lamin A and frequent deformed nuclei in comparison with wild-type mice (Fig. S4), which also implies that the AIMP3-dependent reduction in lamin A is associated with the progeroid phenotype.

To confirm further whether AIMP3 could specifically influence the cellular level of lamin A, we introduced different amounts of AIMP3 into HeLa cells and determined their effect on nuclear lamins. The introduction of AIMP3 reduced the level of lamin A, but not that of prelamin A, lamin B or lamin C (Fig. 3d). Notably, the level of prelamin A increased upon AIMP3 transfection, which might reflect a compensatory attempt to increase the expression of the *LMNA* gene in response to the reduction in lamin A levels that was induced by AIMP3. Thus, the consequence of enhanced expression of AIMP3 was a dramatic increase in the ratio of prelamin A to mature lamin A. We also introduced AIMP3 into p53^{+/+} and p53^{-/-} HCT116 cells and analyzed the change in the level of lamin A. Lamin A levels

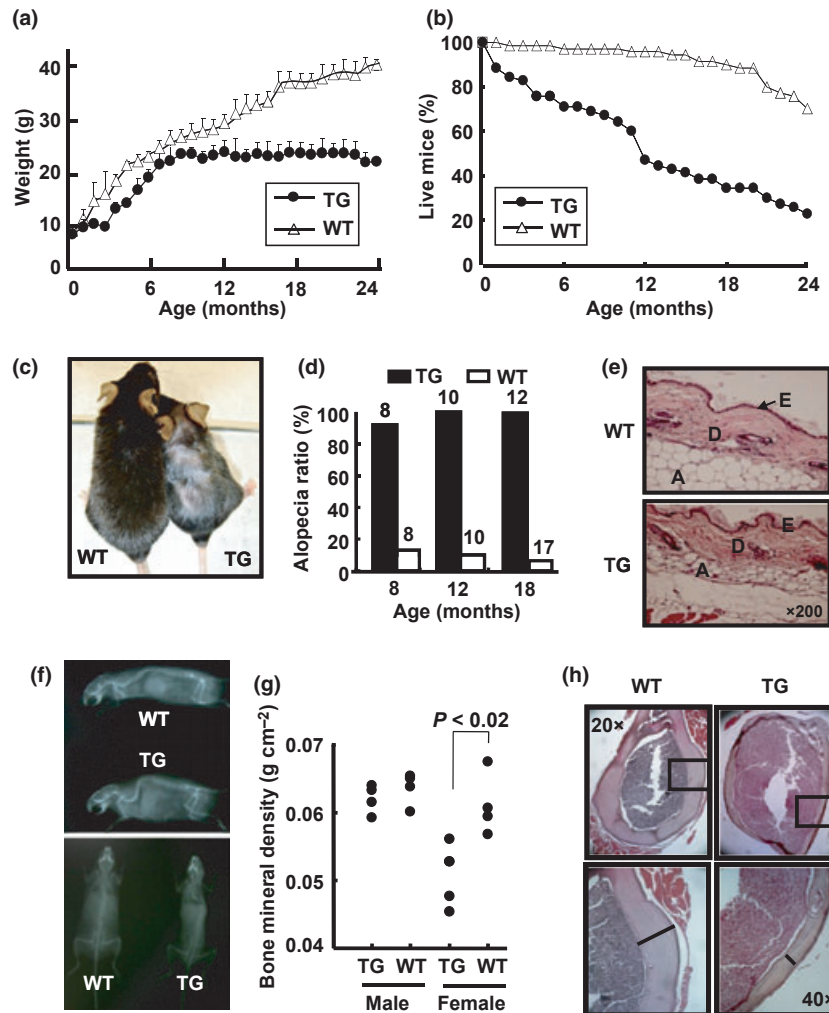


Fig. 2 Progeroid phenotype of AIMP3 transgenic mice. (a) The growth of AIMP3 WT and TG mice ($n = 70$ for each group) was monitored by measuring body weight every 2 weeks for 24 months. The number of AIMP3 transgenic mice decreased gradually as they aged. (b) The survival of AIMP3 WT and TG mice ($n = 70$) was determined by counting the number of live mice every month. (c) Photograph of 10-month-old AIMP3 WT and TG mice. The transgenic mice show alopecia. (d) The number of mice affected by alopecia was determined at the indicated age. (e) The dermal histology of AIMP3 WT and TG mice was examined by hematoxylin and eosin staining. E, D, and A stand for epidermis, dermis, and adipocytes, respectively. The skin of the TG mouse showed apparent wrinkles and reduced subcutaneous fat. (f) Whole-body radiograph of 18-month-old WT and TG mice. The AIMP3 TG mice demonstrated pronounced lordokyphosis. (g) Bone mineral contents (g cm^{-2}) of WT and TG mice are shown and compared ($n = 8$ for each group). (h) Hematoxylin and eosin stained cross-sections of bone from 18-month-old WT and TG mice revealed the reduction in cortical bone thickness of the tibia in AIMP3 TG mice.

decreased in response to increased AIMP3 independently of p53 (Fig. 3e). Conversely, knockdown of AIMP3 increased the levels of lamin A in two different cell lines (HEK 293 and HeLa) that expressed GFP-lamin A (Fig. 3f).

AIMP3 mediates ubiquitin-dependent degradation of lamin A

Given that the level of AIMP3 was correlated inversely with that of lamin A, we transfected the plasmid for AIMP3 into 293 cells and examined using RT-PCR whether transcription of lamin A was affected. The expression of lamin A was not increased by the exogenous introduction of AIMP3 (Fig. S5a), which implies that the downregulation of lamin A induced by AIMP3 may take

place at the post-transcriptional stage. We investigated subsequently whether AIMP3 interacted with lamin A to mediate the degradation of lamin A. To test this possibility, we immunoprecipitated endogenous AIMP3 from 293 cells, and co-precipitation of lamin A was analyzed by western blotting. Under these conditions, we found that AIMP3 was co-precipitated with lamin A (Fig. 4a). Similarly, interaction between the two proteins was also observed by co-immunoprecipitation of GFP-lamin A and GST-AIMP3 in 293 cells (Fig. 4b).

Cellular levels of lamin A are thought to be controlled at the post-transcriptional stage by different mechanisms. First, we tested whether AIMP3 can induce caspase 6-dependent cleavage of lamin A (Broers *et al.*, 2002; Ruchaud *et al.*, 2002). The proteolytic cleavage product of lamin A was detected in the

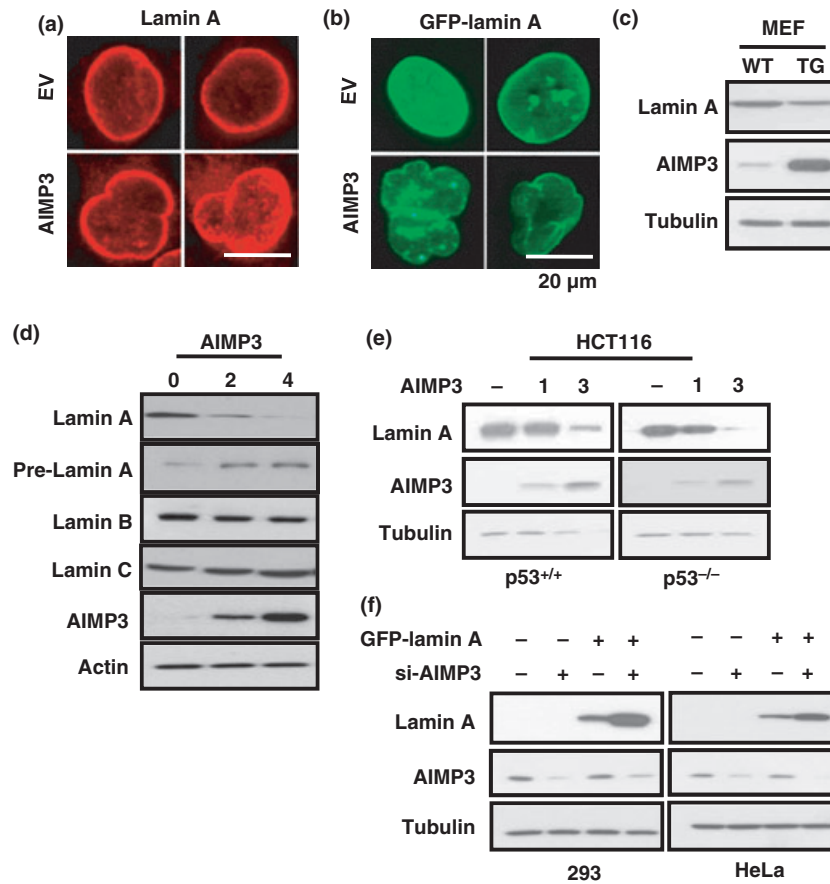


Fig. 3 AIMP3 induces nuclear deformation via specific downregulation of lamin A. (a) HeLa cells were transfected with empty vector (EV) or the AIMP3 expression construct, and nuclear morphologies were compared by immunofluorescence staining of lamin A using anti-lamin A antibody as the primary antibody and Alexa555-conjugated secondary antibody. Approximately 1000 cells from the EV or AIMP3 transfectants were counted and two representative cells are shown. (b) The GFP-lamin A expression construct was co-transfected with EV or the AIMP3 expression construct into HeLa cells, and localization of lamin A was monitored by green fluorescence. Two representative cells are shown out of a total of approximately 1000 cells counted. (c) Cellular levels of lamin A and AIMP3 were determined in AIMP3 WT and TG mouse embryonic fibroblasts by western blotting with an antibody that reacted specifically with lamin A (Santa Cruz H102) and anti-AIMP3 antibody, respectively. (d) The expression construct for Myc-AIMP3 was transfected into HeLa cells at the indicated concentrations ($\mu\text{g mL}^{-1}$), and its effect on the cellular levels of lamin A, prelamin A, lamin B, and lamin C was determined using antibodies that were specific to these proteins. (e) The AIMP3 expression construct was transfected into $p53^{+/+}$ and $p53^{-/-}$ HCT116 cells at the indicated concentration ($\mu\text{g mL}^{-1}$), and the change in the level of lamin A was determined by western blotting. (f) The effect of knockdown of AIMP3 with its specific siRNA on the lamin A level was monitored by western blotting in 293 and HeLa cells. The GFP-lamin A expression construct was transfected into the two cell lines, and the level of expression was determined by western blotting with anti-GFP antibody.

control 293 cells when they were treated with the inhibitor of *de novo* protein synthesis, cycloheximide (Fig. S5a, left three lanes). However, the caspase-dependent cleavage of lamin A was not observed, despite the fact that the level of lamin A decreased more rapidly in the presence of exogenous AIMP3 than in its absence (Fig. S5b, right three lanes). These results suggest that the AIMP3-dependent downregulation of lamin A may occur by a route separate from the cleavage mediated by caspase 6. We also examined the possible degradation of lamin A via the lysosomal pathway. When cells were treated with NH_4Cl , which inhibits lysosome activity, AIMP3-dependent degradation of lamin A was unaffected (Fig. S5c). Thus, it was unlikely that lamin A was degraded via lysosomes.

Another possibility was that lamin A might be degraded through the ubiquitin-dependent proteasome pathway. There-

fore, we tested whether AIMP3-dependent destabilization of lamin A involves ubiquitination. When AIMP3 was introduced into HCT116 $p53^{-/-}$ cells, the cellular level of GFP-lamin A was decreased significantly (Fig. 4c, left two lanes), but it was not affected when the cells were treated with MG132, which blocks proteasome activity (Fig. 4c, right two lanes). These results suggest that AIMP3 may induce ubiquitin-dependent degradation of lamin A. Therefore, we examined whether AIMP3 actually enhances the ubiquitination of lamin A. Ubiquitination of endogenous lamin A was increased when $p53^{-/-}$ HCT116 cells were treated with MG132 and supplemented exogenously with AIMP3 (Fig. 4d). We also transfected $p53^{-/-}$ HCT116 cells with the expression constructs for GFP-lamin A and HA-ubiquitin, treated them with MG132, and then monitored the effect of AIMP3 on ubiquitination of GFP-lamin A. Ubiquitination of

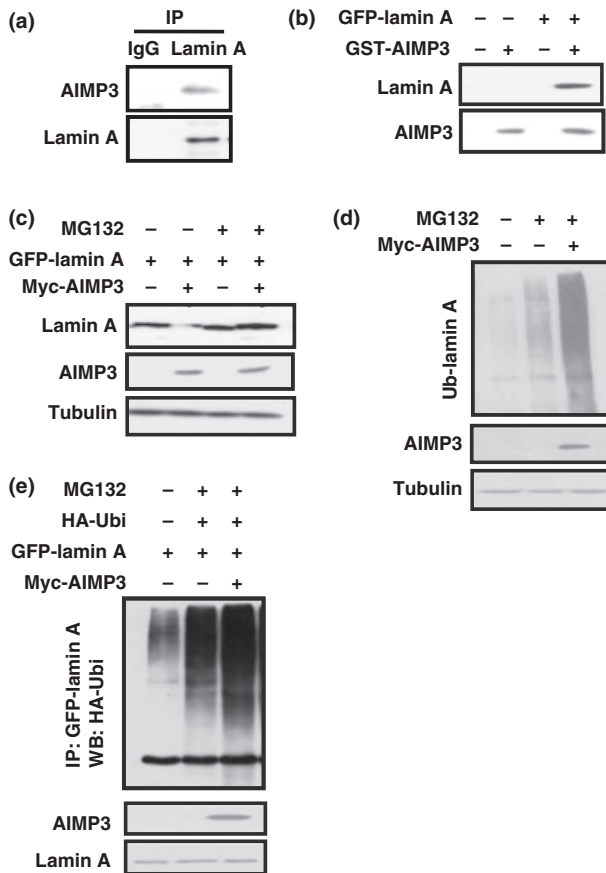


Fig. 4 AIMP3 binds specifically to and reduces the cellular level of lamin A via ubiquitin-mediated degradation. (a) The interaction of endogenous AIMP3 with lamin A was determined by co-immunoprecipitation. Proteins extracted from 293 cells were immunoprecipitated with anti-lamin A antibody, and co-precipitation of AIMP3 was determined by western blotting. (b) The expression constructs for GFP-lamin A and GST-AIMP3 were transfected into 293 cells in the indicated combinations, and GST-AIMP3 was immunoprecipitated with glutathione-Sepharose. Co-precipitation of GFP-lamin A was analyzed by western blotting with the anti-GFP antibody. (c) p53^{-/-} HCT116 cells were transfected with the indicated plasmids expressing Myc-AIMP3 and GFP-lamin A, treated with MG132 for 6 h, and the cell lysates were analyzed by western blotting with anti-Myc and anti-GFP antibodies, respectively. (d) p53^{-/-} HCT116 cells transfected with EV or the Myc-AIMP3 expression construct were treated with MG132 and subjected to immunoprecipitation with anti-lamin A antibody. The precipitates were separated by SDS-PAGE, and ubiquitinated lamin A was detected by western blotting with anti-ubiquitin antibody. (e) p53^{-/-} HCT116 cells expressing HA-ubiquitin, Myc-AIMP3, and GFP-lamin A were grown in the absence and presence of MG132. The cell lysates were immunoprecipitated with anti-GFP antibody, and the precipitates were immunoblotted with anti-HA antibody.

GFP-lamin A with HA-ubiquitin was increased by the introduction of AIMP3 (Fig. 4e). We also examined whether AIMP3 is involved specifically in the ubiquitination of lamin A. To address this question, we transfected 293 cells with an expression vector for AIMP2, which is another cofactor that is associated with the multi-tRNA synthetase complex (Kim *et al.*, 2002a), and compared its effect on the level of lamin A with that of AIMP3. In contrast to AIMP3, AIMP2 did not reduce the level of lamin A (Fig. S5c), which suggests a specific involvement of AIMP3 in the control of lamin A levels. Taken together, these results sug-

gest that AIMP3 can control the cellular levels of lamin A via ubiquitination.

AIMP3-mediated ubiquitination of lamin A involves Siah1

The E3 ubiquitin ligase, Siah1, has been suggested to catalyze the ubiquitination of lamin A (Depaux *et al.*, 2006; Winter *et al.*, 2008). We tested whether the ubiquitination of lamin A that is induced by AIMP3 involves Siah1. First, we checked whether the level of lamin A was affected by the combination of Siah1 and AIMP3. Whereas the level of lamin A was decreased by the introduction of Siah1, as expected, the addition of AIMP3 augmented the effect of Siah1 further (Fig. 5a), which suggests a cooperative effect of the two proteins on the downregulation of lamin A. We transfected the plasmid for AIMP3 and reduced Siah1 levels by siRNA simultaneously and found that the ubiquitination of lamin A mediated by AIMP3 was reduced by knock-down of Siah1 (Fig. 5b). Similarly, the Siah1-dependent ubiquitination of lamin A was decreased in a dose-dependent manner when the expression of AIMP3 was suppressed by siRNA (Fig. 5c). We investigated subsequently the interaction between Siah1 and AIMP3 by co-immunoprecipitation. As the level of expression of Siah1 increased, its association with Myc-tagged AIMP3 was also enhanced, whereas Siah1 itself was not precipitated with anti-Myc antibody (Fig. 5d). Direct interaction of Siah1 with AIMP3 was confirmed by an *in vitro* pull-down assay that used radioactively labeled Siah1 and GST-AIMP3 (Fig. 5e). We tested whether the binding of Siah1 to lamin A was affected by AIMP3, using a co-immunoprecipitation assay. When the expression of AIMP3 was suppressed by siRNA, the amount of lamin A that was immunoprecipitated with Siah1 decreased (Fig. 5f), which suggests that AIMP3 can bind to both Siah1 and lamin A and may mediate their interaction.

Previously, we have solved the three-dimensional structure of AIMP3 and characterized various point mutations to determine the residues that are important for its molecular interactions and tumor suppressive activity (Kim *et al.*, 2008) (Fig. S6a). In this study, we investigated whether any of these mutations affected the ability of AIMP3 to suppress the level of lamin A. When each of these mutants was introduced into 293 cells and the cellular levels of lamin A compared, we found that the V106A mutant of AIMP3 did not reduce the lamin A level and the R144A mutant showed only a partial reduction in lamin A, whereas the activity of all the other mutants was similar to that of the wild-type AIMP3 (Fig. S6b). Therefore, we compared the effect of the wild-type protein and the V106A mutant on the ubiquitination of lamin A after the introduction of HA-ubiquitin into 293 cells. The V106A mutant had little effect on the ubiquitination of lamin A, in contrast to the wild-type AIMP3 (Fig. S6c). We also examined whether the V106A mutant had lost its ability to bind to lamin A and/or Siah1 by co-immunoprecipitation. Lamin A was not co-precipitated with the V106A mutant, which suggests that the V106 residue is important for the interaction of AIMP3 with lamin A (Fig. S6d). The mutation at V106 also

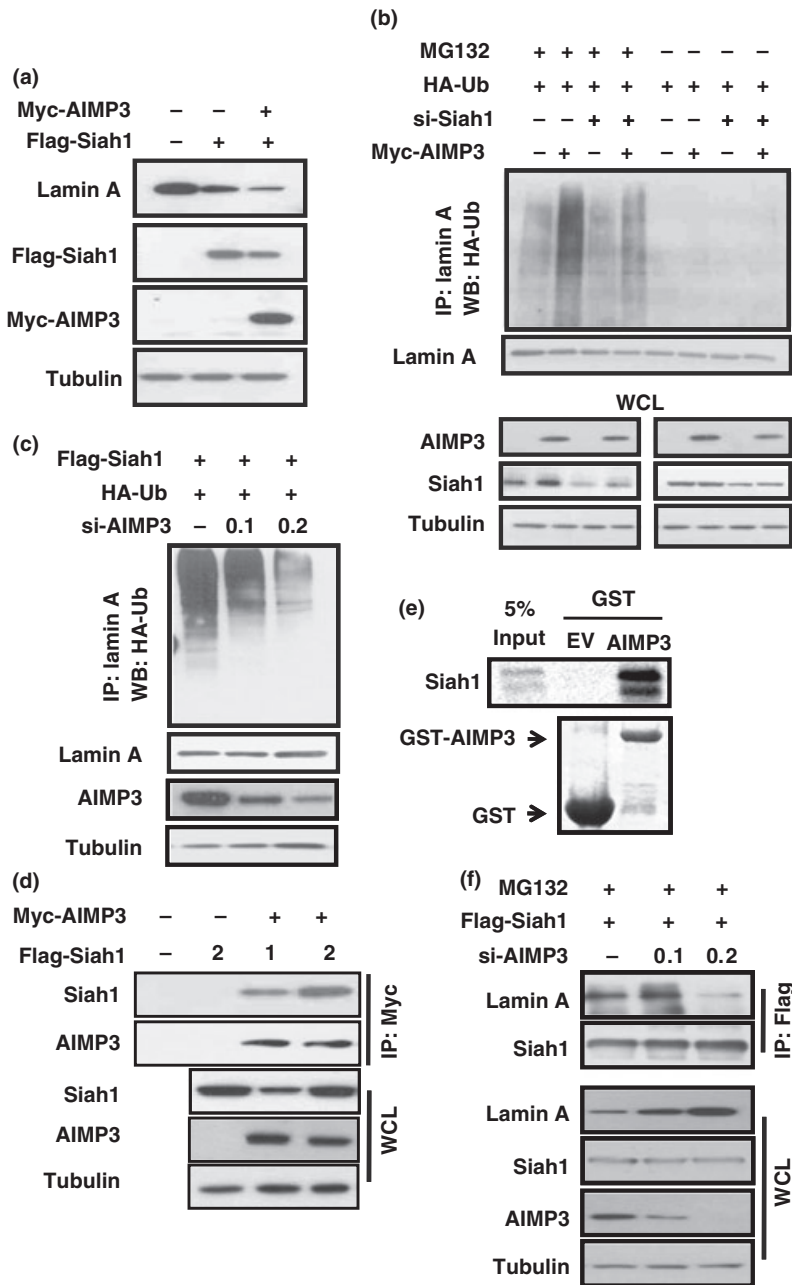


Fig. 5 AIMP3 facilitates Siah1-dependent ubiquitination of lamin A. (a) The FLAG-Siah1 expression construct was transfected into p53^{-/-} HCT116 cells with or without the plasmid for Myc-AIMP3, and after 24 h of incubation, the levels of lamin A, Siah1, and AIMP3 were determined by western blotting with anti-lamin A, anti-FLAG, and anti-Myc antibodies, respectively. Tubulin was included as a loading control. (b) 293 cells were transfected with the indicated combination of HA-ubiquitin, si-Siah1 and Myc-AIMP3 plasmids and further incubated in the absence or presence of MG132 for 10 h. The cell lysates were then immunoprecipitated with anti-lamin A antibody, and the precipitates were immunoblotted with anti-HA antibody. The levels of expression of Myc-AIMP3, Siah1, and tubulin in whole cell lysates (WCL) were determined with anti-Myc, anti-Siah1, and anti-tubulin antibodies, respectively. (c) p53^{-/-} HCT116 cells were transfected with the indicated combination of FLAG-Siah1, HA-ubiquitin, and si-AIMP3 (0, 0.1, and 0.2 μM). Lamin A was immunoprecipitated, and the ubiquitination of lamin A was analyzed by immunoblotting with anti-HA antibody. (d) p53^{-/-} HCT116 cells were transfected with the Myc-AIMP3 expression construct and the indicated amounts of FLAG-Siah1 plasmid (0, 1, and 2 μg mL⁻¹). The cell lysates were immunoprecipitated with anti-Myc antibody, and co-precipitation of Siah1 was detected by immunoblotting with anti-Flag antibody. (e) [³⁵S]-labeled full-length Siah1 was prepared by *in vitro* translation and mixed with GST or GST-AIMP3. GST proteins were precipitated with glutathione-Sepharose, and co-precipitation of Siah1 was analyzed by autoradiography. (f) p53^{-/-} HCT116 cells were transfected with the FLAG-Siah1 expression construct and different amounts of si-AIMP3 (μM). After incubation for 48 h, the cells were harvested and subjected to immunoprecipitation with anti-Flag antibody. Co-precipitation of lamin A with FLAG-Siah1 was determined by western blotting using the anti-lamin A antibody.

appeared to reduce the interaction of AIMP3 with Siah1 slightly. This residue also might be involved partially in the interaction with Siah1. These results not only revealed the region of the AIMP3 peptide that was involved in the interaction with lamin A but also supported further the importance of the binding of AIMP3 to lamin A for Siah1-dependent ubiquitination of lamin A.

It is known that the expression of *LMNA* can also result in the production of a splice variant, termed progerin ($\Delta 50$) (Eriksson

et al., 2003) (Fig. 6a). Specific mutations that result in increased levels of progerin are associated with HGPS. The level of this variant has also been reported to be increased in aged cells of normal individuals that have a corresponding reduction in mature lamin A (Wang et al., 2008). Therefore, we investigated whether AIMP3 also affected the ubiquitination of progerin. Transfection of the AIMP3 expression construct increased the ubiquitination of lamin A, as described earlier, but not that of

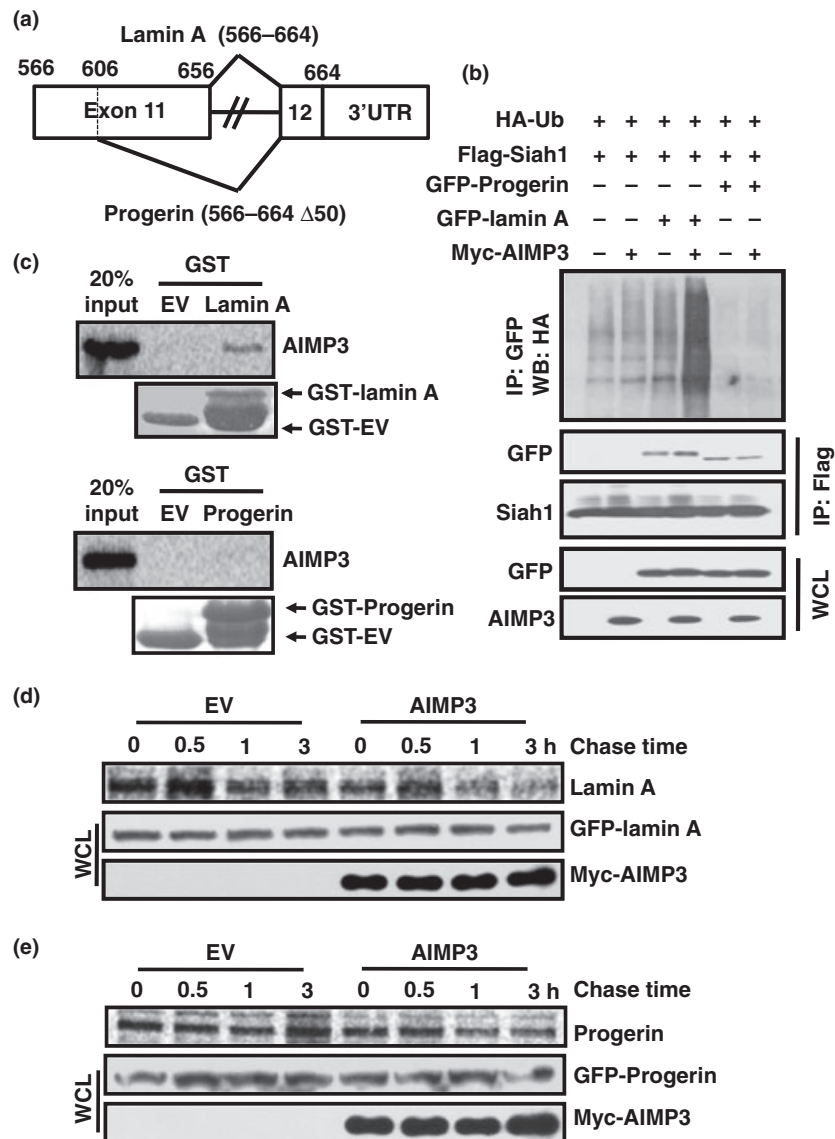


Fig. 6 AIMP3 specifically mediates ubiquitination of lamin A but not of progerin. (a) The difference in the structure of exons 11–12 between lamin A and progerin is shown schematically. The lamin A cDNA consists of 12 exons. Progerin is a form of lamin A that is truncated by 50 aa as the result of an alternative splicing event between the N-terminal regions of exons 11 and 12. (b) 293 cells were transfected with plasmids for HA-ubiquitin, FLAG-Siah1 and the indicated combination of GFP-progerin or GFP-lamin A. AIMP3 and lamin A were immunoprecipitated, and the precipitates were separated by SDS-PAGE. Ubiquitination of lamin A and progerin was determined by immunoblotting with anti-HA antibody. (c) The direct interaction of lamin A and progerin with AIMP3 was analyzed by *in vitro* pull-down assay. Radioactive AIMP3 was synthesized by *in vitro* translation and mixed with GST-lamin A (exon 11–12 fragment) or GST-progerin (Δ exon 11–12). GST proteins were precipitated with glutathione-Sepharose, and co-precipitation of AIMP3 was detected by autoradiography. The effect of AIMP3 on cellular turnover of lamin A (d) and progerin (e) was determined by a pulse-chase experiment. 293 cells were transfected with Myc-AIMP3 and GFP-lamin A or GFP-progerin and labeled with radioactive methionine for 3 h. Cellular protein synthesis was then blocked with cycloheximide, and GFP-lamin A or GFP-progerin was immunoprecipitated with anti-GFP antibody and subjected to autoradiography.

progerin (Fig. 6b). We tested whether AIMP3 bound to progerin as well as to lamin A by an *in vitro* pull-down assay. We prepared GST proteins fused to a fragment of lamin A that spanned exons 11–12 or to the corresponding fragment of progerin (Fig. 6a). These two GST fusion proteins were mixed with radioactively labeled AIMP3 and precipitated with glutathione-Sepharose. The AIMP3 was co-precipitated with GST-lamin A, but not with GST-progerin (Fig. 6c). We also compared the effect of AIMP3 on the rate of cellular turnover of lamin A and progerin using a pulse-chase experiment. Although the levels of lamin A were decreased rapidly following transfection of the AIMP3 expression construct, compared with those in the control cells (Fig. 6d), the levels of progerin were affected little by the introduction of AIMP3 (Fig. 6e). Given that transfection of the plasmid for AIMP3 did not diminish the level of lamin C (Fig. 3d), which also lacks the C-terminal region, we examined the interaction of AIMP3 with different forms of lamin by co-immunoprecipitation. AIMP3 showed specific binding to lamin A, but not to lamin B, C or progerin (Fig. S7). To confirm further the importance of the C-terminal region of lamin A for the interaction with AIMP3, we prepared the L647R mutant of lamin A, which blocks processing of the C-terminus, and determined its ability to bind to AIMP3 using the *in vitro* pull-down assay. The radioactively labeled AIMP3 was co-precipitated with wild-type lamin A, but not with the L647R mutant or progerin (Fig. S7). All of these results indicate that the targeting of lamin A for degradation by AIMP3 requires a region of the C-terminus of lamin A that is lacking in lamin C and progerin. These results support further the importance of the C-terminal extension of progerin/prelamin A in causing progeria (Smallwood & Shackleton, 2010).

Discussion

Our findings indicated that increased expression of AIMP3 promoted senescence in cell culture and the accelerated onset of a range of characteristics that are associated with aging *in vivo*, including cachexia, alopecia, lordokyphosis, reduced bone mineral deposits in females, reduced bone thickness, and mortality itself (Fig. 2). This phenotype overlapped significantly with the murine model of HGPS (Mounkes *et al.*, 2003), which is associated with the expression of a variant of lamin A, progerin, that lacks 50 amino acids at the C-terminus and (unlike mature lamin A) remains fully farnesylated.

Our studies also indicated a direct connection between AIMP3 and lamin A: AIMP3 interacted with lamin A and mediated its degradation through a proteasome-dependent process that involved Siah1. Importantly, progerin and lamin C were immune to degradation mediated by AIMP3 (Figs 3d and 6), presumably because they lacked a region in the C-terminus that is necessary for interaction with AIMP3. Given that mice that lack lamin A specifically and express only lamin C have no robust phenotype (Fong *et al.*, 2006; Scaffidi & Misteli, 2006), it might be expected that overexpression of AIMP3, which would result in a high ratio of lamin C to lamin A, would also lead to the lack of a distinct

phenotype. However, it is likely that the difference is because of the fact that the level of prelamin A increases as a result of overexpression of AIMP3, which leads to high levels of prelamin A relative to mature lamin A. Thus, we propose that AIMP3 transgenic mice closely resemble *Zmpste24*^{-/-} mice, which fail to cleave farnesylated lamin A and manifest a progeroid phenotype similar to that of mice that express progerin. This model predicts that increased expression of lamin A or an enforced reduction in prelamin A might rescue senescence and/or the progeroid phenotype that is associated with overexpression of AIMP3. Consistently, we found that increased expression of lamin A offsets the senescent phenotype that was associated with overexpression of AIMP3 (Fig. S3). In the future, it will be important to test this assertion in murine models of progeria.

Findings from previous studies in both murine models and humans have indicated that AIMP3 acts as a tumor suppressor. It is likely that one mechanism of tumor suppression is mediated through p53 and involves the ability of AIMP3 to protect against DNA damage by activating ATM/ATR. This study suggests a second mechanism of tumor suppression that is independent of p53. Many stimuli that are potentially oncogenic induce senescence, and senescence is a well-recognized, potent mechanism of tumor suppression. However, the effects of senescence against cancer can also be deleterious and may contribute to age-related pathologies, as predicted by evolutionary antagonistic pleiotropy (Campisi & d'Adda di Fagagna, 2007). This is illustrated by the observation that chronically active p53 promotes cellular senescence and accelerates the aging phenotype (Tyner *et al.*, 2002; Maier *et al.*, 2004), as well as by recent studies that suggest a paracrine pro-tumorigenic effect through the release of inflammatory factors (Evan & d'Adda di Fagagna, 2009). We propose that, in addition to the activation of a p53-dependent checkpoint by AIMP3, tumor suppression, through the induction of cell senescence, is linked to elevated levels of farnesylated lamin A relative to mature lamin A. This hypothesis is consistent with the observations of accelerated senescence in HGPS and *Zmpste24*^{-/-} fibroblasts (Smith *et al.*, 2005; Huang *et al.*, 2008). This function of AIMP3 might also involve DNA damage pathways, because models of HGPS are reported to have elevated levels of DNA damage and/or active DNA damage response pathways (Varela *et al.*, 2005; Schumacher *et al.*, 2008a,b). Moreover, the premature mortality of *Zmpste24*^{-/-} mice is rescued partly by the loss of p53 (Varela *et al.*, 2005; Navarro *et al.*, 2006; Kudlow *et al.*, 2008), which suggests that DNA damage response pathways might also be involved in the senescence program associated with the expression of prelamin A.

Loss of A-type lamins is also associated with decreased function of retinoblastoma protein (pRB), either through decreased stability or through hyperphosphorylation (Markiewicz *et al.*, 2002; Johnson *et al.*, 2004; Van Berlo *et al.*, 2005; Nitta *et al.*, 2007; Pekovic *et al.*, 2007). As a consequence, *Lmna*^{-/-} mouse fibroblasts have altered cell cycle kinetics that are similar to those of *Rb*^{-/-} fibroblasts; the overall transit time of *Lmna*^{-/-} mouse fibroblasts through the cell cycle is not altered, but the

cells spend reduced time in G1-phase and exhibit a compensatory increase in S-phase (Nitta *et al.*, 2007). It will be of interest to determine the levels of pRB in cells that overexpress AIMP3 and also in cells that mimic the relevant state of A-type lamins (prelamin A and lamin C, but no lamin A) to determine the potential role of altered activation of pRB and its possible links to cell senescence and tumor suppression.

Previously, we have shown that lower expression of AIMP3 confers higher susceptibility to tumorigenesis in mice, and hypomorphic mutations or allelic deletions of the AIMP3-encoding gene have been found in patients with cancer. In this study, we found that increased expression of AIMP3 can cause cellular senescence and promote the progeroid phenotype, which suggests that the cellular level of AIMP3 should be controlled tightly. In normal cells, AIMP3 is sequestered mainly within the multi-tRNA synthetase complex (Quevillon & Mirande, 1996; Han *et al.*, 2006). This cytosolic macromolecular complex might provide a molecular repository that can buffer temporary or aberrant fluctuations in the cellular level of this critical factor. A better understanding of how the level and localization of AIMP3 are modulated in normal mice and of how this affects the relative levels of the isoforms of A-type lamin will be an important future goal.

Progerias are segmental in nature and recapitulate only a subset of the phenotypic changes that are associated with normal aging (Smith *et al.*, 2005; Schumacher *et al.*, 2008b), and it has been debated whether the genetic changes that cause progeria also affect normal aging (Martin & Oshima, 2000; Miller, 2004; Kudlow *et al.*, 2007). Interestingly, several studies have reported the presence of an altered splice form of lamin A, identical to progerin, that either accumulates with age or remains constant but has an impact on the senescent phenotype in cell culture (Martin & Oshima, 2000; Smith *et al.*, 2005; Broers *et al.*, 2006). These studies have led to the hypothesis that progerin is involved in the normal aging process. Herein, we have reported that lamin A is degraded more rapidly in mice that overexpress AIMP3 than in wild-type mice, but that the stability of progerin should remain intact (Fig. 6). Although this phenotype has been observed in transgenic mice, which have enforced overexpression of AIMP3, the endogenous levels of AIMP3 can vary depending on the cell cycle phase or in response to DNA damage (Park *et al.*, 2005b). We found that the level of endogenous AIMP3 also showed a gradual increase, with a concurrent decrease in lamin A, as the passage number of human skin fibroblasts increased (Fig. S8). We also compared the levels of AIMP3 and lamin A in the human tissues of different ages and observed a similar pattern to that described elsewhere (Fig. S8). Although further investigation and case studies are needed, these results support further the possible role of AIMP3 in the normal human aging process via the regulation of lamin A. The findings of this work, together with those of our previous reports, show that AIMP3 appears to play a pivotal role in the delicate connection between aging and cancer.

Methods

Materials and transfection

Mammalian expression vectors for lamin A and progerin were generously provided by Tom Misteli (NIH/NCI). The HA-ubiquitin and FLAG-Siah1 expression vectors were kind gifts of Drs I. K. Chung (Yonsei University) and Ze'ev Ronai (Burnham Institute), respectively. For transfection, we used the Lipofectamine system, following the manufacturer's protocol. Cells were transfected with expression constructs for the different types of lamin, incubated for 24 h or the indicated time, treated with 10 μ M MG132 for 6 h, and harvested with radioimmunoprecipitation assay (RIPA) buffer. The L647R mutant of lamin A was generated via site-directed mutagenesis using a QuikChange kit (Stratagene, Agilent, USA). Proteins extracted from the cells were separated by SDS-PAGE and subjected to western blot analysis with the indicated antibodies. The specific antibodies for prelamin A (C-20), lamin A (H-102), ubiquitin (P4D1), and lamin B (M-20) were purchased from Santa Cruz Biotechnology (California, USA) and the antibody that recognized both lamin A and lamin C (#2032) was from Cell Signaling (Beverly MA, USA). The anti-p16 antibody was also obtained from Cell Signaling and the antibodies against DcR2 and GFP were from Santa Cruz Biotechnology. The anti-AIMP3 antibody (AbCam, Cambridge, UK) was described previously (Park *et al.*, 2005a). The ECL solution (WEST-one) for western blotting was purchased from Intron Biotechnology (Seoul, Korea). For the knockdown of AIMP3 and Siah1, the cells were transfected with AIMP3 siRNA (5'-CCAAGUCUAACAGGAUUGACUACUA-3'), Siah1 siRNA (sc-37495, Santa Cruz Biotechnology) or universal siRNA as the control using Lipofectamine 2000 (Invitrogen, KDR, Korea), following the manufacturer's instructions, and incubated for 48 h before further analyses.

Cell culture

The HEK 293 and Hela cells were grown in DMEM (Hyclone) plus 10% fetal bovine serum at 37 °C. The PC3, HCT116 p53^{+/+}, and HCT116 p53^{-/-} cells were grown in RPMI (Hyclone) that contained 10% fetal bovine serum, with 2% penicillin and streptomycin. Embryonic 12.5d AIMP3 wild-type and transgenic MEFs were established in DMEM (Hyclone, Seoul Bioscience, Korea) that contained 10% fetal bovine serum, with 2% penicillin and streptomycin. Cells of passage numbers from 2 to 5 were used for the experiments.

Generation of AIMP3 transgenic mice

To generate AIMP3 transgenic mice, the full-length murine AIMP3 cDNA, which encodes 234 amino acids, was obtained by RT-PCR using murine transcripts as a template and subcloned into the *EcoRI* site of the pCAGGS expression vector. This vector contains a human cytomegalovirus immediate-early enhancer linked to the chicken- β -actin promoter (Niwa *et al.*, 1991). The

inserted fragment was cut from the vector with *Sall* and *HindIII*, and the purified DNA was microinjected into the pro-nuclei of fertilized eggs from FVB/N mice, which were then transferred to pseudopregnant female FVB/N mice. Founder genotypes were determined by PCR of DNA isolated from the tails of the mice with primers specific to the inserted DNA sequence (Fig. S1a). Three founders were established. First-generation heterozygote transgenic offspring were obtained by backcrossing the founders with C57Bl/6J mice. The expression of AIMP3 in the transgenic mice was confirmed by immunoblotting and RT-PCR. All the experiments were performed in the Association for Assessment and Accreditation of Laboratory Animal Care certified facility, in compliance with animal policies approved by Sungkyunkwan University School of Medicine.

Phenotype analysis

Lordokyphosis was monitored by whole-body X-ray analysis *in situ* at a dose of 20 kV for 20 s under anesthesia. Bone thickness and mineral content were analyzed using the tibia, as described previously (Ducy *et al.*, 1996). Dorsal skin sections were fixed, embedded in paraffin, and stained with hematoxylin and eosin. The thickness of the dermal and adipose layers from the skin samples was determined by taking eight random measurements along the length of individual skin samples ($n = 4$) for each genotype and age group.

β -galactosidase staining

Cells were washed once with PBS (pH 7.2), fixed with PBS containing 0.5% glutaraldehyde, washed again with PBS supplemented with 1 mM MgCl₂, and stained in X-gal solution (Senescence β -Galactosidase Staining kit; Cell Signaling Technology) overnight at 37 °C.

Fluorescence staining

HeLa cells were seeded on a cover glass and transfected with the plasmid for lamin A. After fixation with methanol, the glass was incubated with blocking buffer (PBS containing 0.01% bovine serum albumin and 0.05% Triton X-100) for 1 h. After washing with PBST, the cells were incubated with the primary antibody (1:200) and then with the Alexa555-conjugated secondary antibody (1:300). The cells were stained with DAPI. Cells that expressed GFP-lamin A were examined by fluorescence microscopy after transfection at $\times 40$ magnification using a confocal microscope (μ -Radiance; Bio-Rad, Seoul, Korea). To quantify abnormal nuclear morphology, HeLa cell nuclei were examined in two independent experiments, and the results were displayed graphically.

Western blotting and co-immunoprecipitation

The cells were lysed in RIPA buffer that contained a protease inhibitor cocktail, and the lysates were centrifuged at 16000 g

for 30 min. To examine the interaction between AIMP3 and lamin A, the protein extracts were incubated with normal IgG and protein A/G agarose for 2 h and centrifuged to remove nonspecific IgG-binding proteins. After centrifugation, we collected the supernatants, added the antibody against lamin A (2 μ g per sample), incubated the samples for 2 h at 4 °C, and added protein A/G agarose. After washing twice with ice-cold PBS and once with RIPA, the precipitates were dissolved in SDS sample buffer and separated by SDS-PAGE. The proteins were transferred to PVDF (polyvinylidene fluoride) membrane, and AIMP3 was detected by incubation with the anti-AIMP3 monoclonal antibody followed by horseradish peroxidase-conjugated secondary antibody.

In vitro pull-down assay

GST-lamin A and GST-progerin were mixed with glutathione-Sepharose in PBS that contained 1% Triton X-100 and 0.5% *N*-laurylsarcosine at 4 °C for 2 h. AIMP3 was synthesized by *in vitro* translation in the presence of [³⁵S] methionine using the TNT Quick Coupled Transcription/Translation system (Promega, USA). The synthesized peptide was added to the GST protein mixture mentioned earlier, incubated at 4 °C for 4 h with rotation in PBS that contained 1% Triton X-100, 0.5% *N*-lauroylsarcosine, 1 mM DTT, 2 mM EDTA, and 300 μ M phenylmethylsulfonyl fluoride, and washed six times with the same buffer but with 0.5% Triton X-100. We then eluted the proteins bound to the Sepharose beads with SDS sample buffer, separated them by SDS-PAGE, and autoradiographed the resulting gel.

Acknowledgments

We thank Tom Misteli (NIH/NCI) and Chan Soo Shin for the lamin A and progerin and GFP expression vectors, respectively. This work was supported by the grants of Acceleration Research (2009-0063498), of the 21th Frontier Functional Proteomics Research (FPR0881-250), of the WCU project (R31-2008-000-10103-0) from Ministry of Education, Science and Technology, and of the Korea Healthcare Technology (A092255-0911-1110100) from Ministry of Health and Welfare Affairs and from Gyeonggi-do.

References

- Agarwal AK, Fryns JP, Auchus RJ, Garg A (2003) Zinc metalloproteinase, ZMPSTE24, is mutated in mandibuloacral dysplasia. *Hum. Mol. Genet.* **12**, 1995–2001.
- Broers JL, Bronnenberg NM, Kuijpers HJ, Schutte B, Hutchison CJ, Ramaekers FC (2002) Partial cleavage of A-type lamins concurs with their total disintegration from the nuclear lamina during apoptosis. *Eur. J. Cell Biol.* **81**, 677–691.
- Broers JL, Ramaekers FC, Bonne G, Yaou RB, Hutchison CJ (2006) Nuclear lamins: laminopathies and their role in premature ageing. *Physiol. Rev.* **86**, 967–1008.
- Campisi J, d'Adda di Fagnana F (2007) Cellular senescence: when bad things happen to good cells. *Nat. Rev. Mol. Cell Biol.* **8**, 729–740.

- Collado M, Gil J, Efeyan A, Guerra C, Schuhmacher AJ, Barradas M, Benguria A, Zaballos A, Flores JM, Barbacid M, Beach D, Serrano M (2005) Tumour biology: senescence in premalignant tumours. *Nature* **436**, 642.
- Collado M, Blasco MA, Serrano M (2007) Cellular senescence in cancer and aging. *Cell* **130**, 223–233.
- De Sandre-Giovannoli A, Bernard R, Cau P, Navarro C, Amiel J, Boccaccio I, Lyonnet S, Stewart CL, Munnich A, Le Merrer M, Levy N (2003) Lamin A truncation in Hutchinson–Gilford progeria. *Science* **300**, 2055.
- Dechat T, Pflieger K, Sengupta K, Shimi T, Shumaker DK, Solimando L, Goldman RD (2008) Nuclear lamins: major factors in the structural organization and function of the nucleus and chromatin. *Genes Dev.* **22**, 832–853.
- Depaux A, Regnier-Ricard F, Germani A, Varin-Blank N (2006) Dimerization of hSiah proteins regulates their stability. *Biochem. Biophys. Res. Commun.* **348**, 857–863.
- Dimri GP, Lee X, Basile G, Acosta M, Scott G, Roskelley C, Medrano EE, Linskens M, Rubelj I, Pereira-Smith O (1995) A biomarker that identifies senescent human cells in culture and in aging skin in vivo. *Proc. Natl Acad. Sci. USA* **92**, 9363–9367.
- Ducy P, Desbois C, Boyce B, Pinero G, Story B, Dunstan C, Smith E, Bonadio J, Goldstein S, Gundberg C, Bradley A, Karsenty G (1996) Increased bone formation in osteocalcin-deficient mice. *Nature* **382**, 448–452.
- Eriksson M, Brown WT, Gordon LB, Glynn MW, Singer J, Scott L, Erdos MR, Robbins CM, Moses TY, Berglund P, Dutra A, Pak E, Durkin S, Csoka AB, Boehnke M, Glover TW, Collins FS (2003) Recurrent de novo point mutations in lamin A cause Hutchinson–Gilford progeria syndrome. *Nature* **423**, 293–298.
- Evan GI, d'Adda di Fagnagna F (2009) Cellular senescence: hot or what? *Curr. Opin. Genet. Dev.* **19**, 25–31.
- Fisher DZ, Chaudhary N, Blobel G (1986) cDNA sequencing of nuclear lamins A and C reveals primary and secondary structural homology to intermediate filament proteins. *Proc. Natl Acad. Sci. USA* **83**, 6450–6454.
- Fong LG, Ng JK, Lammerding J, Vickers TA, Meta M, Cote N, Gavino B, Qiao X, Chang SY, Young SR, Yang SH, Stewart CL, Lee RT, Bennett CF, Bergo MO, Young SG (2006) Prelamin A and lamin A appear to be dispensable in the nuclear lamina. *J. Clin. Invest.* **116**, 743–752.
- Han JM, Lee MJ, Park SG, Lee SH, Razin E, Choi EC, Kim S (2006) Hierarchical network between the components of the multi-tRNA synthetase complex: implications for complex formation. *J. Biol. Chem.* **281**, 38663–38667.
- Huang S, Risques RA, Martin GM, Rabinovitch PS, Oshima J (2008) Accelerated telomere shortening and replicative senescence in human fibroblasts overexpressing mutant and wild-type lamin A. *Exp. Cell Res.* **314**, 82–91.
- Johnson BR, Nitta RT, Frock RL, Mounkes L, Barbie DA, Stewart CL, Harlow E, Kennedy BK (2004) A-type lamins regulate retinoblastoma protein function by promoting subnuclear localization and preventing proteasomal degradation. *Proc. Natl Acad. Sci. USA* **101**, 9677–9682.
- Kim JY, Kang YS, Lee JW, Kim HJ, Ahn YH, Park H, Ko YG, Kim S (2002a) p38 is essential for the assembly and stability of macromolecular tRNA synthetase complex: implications for its physiological significance. *Proc. Natl Acad. Sci. USA* **99**, 7912–7916.
- Kim SW, Cheong C, Sohn YC, Goo YH, Oh WJ, Park JH, Joe SY, Kang HS, Kim DK, Kee C, Lee JW, Lee HW (2002b) Multiple developmental defects derived from impaired recruitment of ASC-2 to nuclear receptors in mice: implication for posterior lenticonus with cataract. *Mol. Cell. Biol.* **22**, 8409–8414.
- Kim KJ, Park MC, Choi SJ, Oh YS, Choi EC, Cho HJ, Kim MH, Kim SH, Kim DW, Kim S, Kang BS (2008) Determination of three dimensional structure and residues of novel tumor suppressor, AIMP3/p18, required for the interaction with ATM. *J. Biol. Chem.* **283**, 14032–14040.
- Kudlow BA, Kennedy BK, Monnat Jr RJ (2007) Werner and Hutchinson–Gilford progeria syndromes: mechanistic basis of human progeroid diseases. *Nat. Rev. Mol. Cell Biol.* **8**, 394–404.
- Kudlow BA, Stanfel MN, Burtner CR, Johnston ED, Kennedy BK (2008) Suppression of proliferative defects associated with processing-defective lamin A mutants by hTERT or inactivation of p53. *Mol. Biol. Cell* **19**, 5238–5248.
- Maier B, Gluba W, Bernier B, Turner T, Mohammad K, Guise T, Sutherland A, Thorner M, Scoble H (2004) Modulation of mammalian life span by the short isoform of p53. *Genes Dev.* **18**, 306–319.
- Markiewicz E, Dechat T, Foisner R, Quinlan RA, Hutchison CJ (2002) Lamin A/C binding protein LAP2alpha is required for nuclear anchorage of retinoblastoma protein. *Mol. Biol. Cell* **13**, 4401–4413.
- Martin GM, Oshima J (2000) Lessons from human progeroid syndromes. *Nature* **408**, 263–266.
- McKeon FD, Kirschner MW, Caput D (1986) Homologies in both primary and secondary structure between nuclear envelope and intermediate filament proteins. *Nature* **319**, 463–468.
- Miller RA (2004) 'Accelerated aging': a primrose path to insight? *Aging Cell* **3**, 47–51.
- Mounkes LC, Kozlov S, Hernandez L, Sullivan T, Stewart CL (2003) A progeroid syndrome in mice is caused by defects in A-type lamins. *Nature* **423**, 298–301.
- Navarro CL, De Sandre-Giovannoli A, Bernard R, Boccaccio I, Boyer A, Genevieve D, Hadj-Rabia S, Gaudy-Marqueste C, Smitt HS, Vabres P, Faivre L, Verloes A, Van Essen T, Flori E, Hennekam R, Beemer FA, Laurent N, Le Merrer M, Cau P, Levy N (2004) Lamin A and ZMPSTE24 (FACE-1) defects cause nuclear disorganization and identify restrictive dermopathy as a lethal neonatal laminopathy. *Hum. Mol. Genet.* **13**, 2493–2503.
- Navarro CL, Cau P, Levy N (2006) Molecular bases of progeroid syndromes. *Hum. Mol. Genet.* **15 Spec No 2**, R151–R161.
- Nitta RT, Smith CL, Kennedy BK (2007) Evidence that proteasome-dependent degradation of the retinoblastoma protein in cells lacking A-type lamins occurs independently of gankyrin and MDM2. *PLoS ONE* **2**, e963.
- Niwa H, Yamamura K, Miyazaki J (1991) Efficient selection for high-expression transfectants with a novel eukaryotic vector. *Gene* **108**, 193–199.
- Park BJ, Kang JW, Lee SW, Choi SJ, Shin YK, Ahn YH, Choi YH, Choi D, Lee KS, Kim S (2005a) The haploinsufficient tumor suppressor p18 upregulates p53 via interactions with ATM/ATR. *Cell* **120**, 209–221.
- Park SG, Ewalt KL, Kim S (2005b) Functional expansion of aminoacyl-tRNA synthetases and their interacting factors: new perspectives on housekeepers. *Trends Biochem. Sci.* **30**, 569–574.
- Park BJ, Oh YS, Park SY, Choi SJ, Rudolph C, Schlegelberger B, Kim S (2006) AIMP3 haploinsufficiency disrupts oncogene-induced p53 activation and genomic stability. *Cancer Res.* **66**, 6913–6918.
- Park SG, Schimmel P, Kim S (2008) Aminoacyl tRNA synthetases and their connections to disease. *Proc. Natl Acad. Sci. USA* **105**, 11043–11049.
- Pekovic V, Harborth J, Broers JL, Ramaekers FC, van Engelen B, Lamens M, von Zglinicki T, Foisner R, Hutchison C, Markiewicz E (2007) Nucleoplasmic LAP2alpha-lamin A complexes are required to maintain a proliferative state in human fibroblasts. *J. Cell Biol.* **176**, 163–172.

- Pendas AM, Zhou Z, Cadinanos J, Freije JM, Wang J, Hultenby K, Astudillo A, Wernerson A, Rodriguez F, Tryggvason K, Lopez-Otin C (2002) Defective prelamin A processing and muscular and adipocyte alterations in Zmpste24 metalloproteinase-deficient mice. *Nat. Genet.* **31**, 94–99.
- Quevillon S, Mirande M (1996) The p18 component of the multisynthetase complex shares a protein motif with the beta and gamma subunits of eukaryotic elongation factor 1. *FEBS Lett.* **395**, 63–67.
- Reid TS, Terry KL, Casey PJ, Beese LS (2004) Crystallographic analysis of CaaX prenyltransferases complexed with substrates defines rules of protein substrate selectivity. *J. Mol. Biol.* **343**, 417–433.
- Ruchaud S, Korfali N, Villa P, Kottke TJ, Dingwall C, Kaufmann SH, Earnshaw WC (2002) Caspase-6 gene disruption reveals a requirement for lamin A cleavage in apoptotic chromatin condensation. *EMBO J.* **21**, 1967–1977.
- Rusinol AE, Sinensky MS (2006) Farnesylated lamins, progeroid syndromes and farnesyl transferase inhibitors. *J. Cell Sci.* **119**, 3265–3272.
- Scaffidi P, Misteli T (2006) Good news in the nuclear envelope: loss of lamin A might be a gain. *J. Clin. Invest.* **116**, 632–634.
- Schumacher B, Garinis GA, Hoeijmakers JH (2008a) Age to survive: DNA damage and aging. *Trends Genet.* **24**, 77–85.
- Schumacher B, van der Pluijm I, Moorhouse MJ, Kosteus T, Robinson AR, Suh Y, Breit TM, van Steeg H, Niedernhofer LJ, van Ijcken W, Bartke A, Spindler SR, Hoeijmakers JH, van der Horst GT, Garinis GA (2008b) Delayed and accelerated aging share common longevity assurance mechanisms. *PLoS Genet.* **4**, e1000161.
- Shappell SB, Gupta RA, Manning S, Whitehead R, Boeglin WE, Schneider C, Case T, Price J, Jack GS, Wheeler TM, Matusik RJ, Brash AR, Dubois RN (2001) 15S-Hydroxyeicosatetraenoic acid activates peroxisome proliferator-activated receptor gamma and inhibits proliferation in PC3 prostate carcinoma cells. *Cancer Res.* **61**, 497–503.
- Smallwood DT, Shackleton S (2010) Lamin A-linked progerias: is farnesylation the be all and end all? *Biochem. Soc. Trans.* **38**, 281–286.
- Smith ED, Kudlow BA, Frock RL, Kennedy BK (2005) A-type nuclear lamins, progerias and other degenerative disorders. *Mech. Ageing Dev.* **126**, 447–460.
- Sun P, Yoshizuka N, New L, Moser BA, Li Y, Liao R, Xie C, Chen J, Deng Q, Yamout M, Dong MQ, Frangou CG, Yates III JR, Wright PE, Han J (2007) PRAK is essential for ras-induced senescence and tumor suppression. *Cell* **128**, 295–308.
- Swarbrick A, Roy E, Allen T, Bishop JM (2008) Id1 cooperates with oncogenic Ras to induce metastatic mammary carcinoma by subversion of the cellular senescence response. *Proc. Natl Acad. Sci. USA* **105**, 5402–5407.
- Tyner SD, Venkatachalam S, Choi J, Jones S, Ghebraniou N, Igelmann H, Lu X, Soron G, Cooper B, Brayton C, Hee Park S, Thompson T, Karsenty G, Bradley A, Donehower LA (2002) p53 mutant mice that display early ageing-associated phenotypes. *Nature* **415**, 45–53.
- Van Berlo JH, Voncken JW, Kubben N, Broers JL, Duisters R, van Leeuwen RE, Crijns HJ, Ramaekers FC, Hutchison CJ, Pinto YM (2005) A-type lamins are essential for TGF-beta1 induced PP2A to dephosphorylate transcription factors. *Hum. Mol. Genet.* **14**, 2839–2849.
- Varela I, Cadinanos J, Pendas AM, Gutierrez-Fernandez A, Folgueras AR, Sanchez LM, Zhou Z, Rodriguez FJ, Stewart CL, Vega JA, Tryggvason K, Freije JM, Lopez-Otin C (2005) Accelerated ageing in mice deficient in Zmpste24 protease is linked to p53 signalling activation. *Nature* **437**, 564–568.
- Verstraeten VL, Broers JL, Ramaekers FC, van Steensel MA (2007) The nuclear envelope, a key structure in cellular integrity and gene expression. *Curr. Med. Chem.* **14**, 1231–1248.
- Wang Y, Panteleyev AA, Owens DM, Djabali K, Stewart CL, Worman HJ (2008) Epidermal expression of the truncated prelamin A causing Hutchinson–Gilford progeria syndrome: effects on keratinocytes, hair and skin. *Hum. Mol. Genet.* **17**, 2357–2369.
- Winter M, Sombroek D, Dauth I, Moehlenbrink J, Scheuermann K, Crone J, Hofmann TG (2008) Control of HIPK2 stability by ubiquitin ligase Siah-1 and checkpoint kinases ATM and ATR. *Nat. Cell Biol.* **10**, 812–824.

Supporting Information

Additional supporting information may be found in the online version of this article:

Fig. S1 Detection of the insertion of the murine AIMP3 cDNA into murine chromosomes.

Fig. S2 Knockdown of AIMP3 suppresses cellular senescence.

Fig. S3 Exogenous supplementation of lamin A rescues AIMP3-induced senescence.

Fig. S4 The effect of increased expression of AIMP3 on lamin A levels and nuclear structure.

Fig. S5 AIMP3 specifically enhances ubiquitination of lamin A.

Fig. S6 The effect of mutation of AIMP3 on its interaction with lamin A, together with cellular levels and ubiquitination of lamin A.

Fig. S7 The specific interaction of AIMP3 with lamin A.

Fig. S8 Levels of AIMP3 and lamin A in human skin fibroblasts at different passages and in human tissues at different ages.

As a service to our authors and readers, this journal provides supporting information supplied by the authors. Such materials are peer-reviewed and may be re-organized for online delivery but are not copy-edited or typeset. Technical support issues arising from supporting information (other than missing files) should be addressed to the authors.